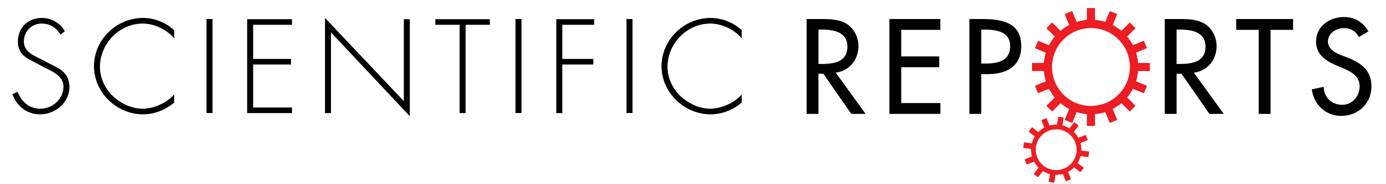

OPEN

A multilevel nonvolatile magnetoelectric memory

Jianxin Shen, Junzhuang Cong, Dashan Shang, Yisheng Chai, Shipeng Shen, Kun Zhai & Young Sun

Received: 25 May 2016
Accepted: 14 September 2016
Published: 29 September 2016

The coexistence and coupling between magnetization and electric polarization in multiferroic materials provide extra degrees of freedom for creating next-generation memory devices. A variety of concepts of multiferroic or magnetoelectric memories have been proposed and explored in the past decade. Here we propose a new principle to realize a multilevel nonvolatile memory based on the multiple states of the magnetoelectric coefficient (α) of multiferroics. Because the states of α depends on the relative orientation between magnetization and polarization, one can reach different levels of α by controlling the ratio of up and down ferroelectric domains with external electric fields. Our experiments in a device made of the PMN-PT/Terfenol-D multiferroic heterostructure confirm that the states of α can be well controlled between positive and negative by applying selective electric fields. Consequently, two-level, four-level, and eight-level nonvolatile memory devices are demonstrated at room temperature. This kind of multilevel magnetoelectric memory retains all the advantages of ferroelectric random access memory but overcomes the drawback of destructive reading of polarization. In contrast, the reading of α is nondestructive and highly efficient in a parallel way, with an independent reading coil shared by all the memory cells.

Ferroelectric random access memory (FeRAM) that stores information by using the spontaneous polarization (*P*) of ferroelectrics is a mature and promising nonvolatile memory because of its high endurance, fast read/write speed, low power consumption, and reliable multilevel polarization states[1–5]. Nonetheless, one major problem associated with conventional FeRAM is on the reading operation. The reading of *P* is usually performed by applying a bias voltage to the ferroelectric capacitor and detecting the *P* switching current. This process is destructive and a rewrite step is necessary. Moreover, this reading method also requires a minimum capacitor size to generate enough current for the sensing circuit, and thus the storage density is limited. Recently, the photovoltaic effect of ferroelectrics such as $BiFeO_3$ has been used to read the *P* direction nondestructively[6]. However, this method is restricted to specific ferroelectric materials with a band gap in the visible range and requires additional light source. Here, we propose and demonstrate that the problem of destructive reading of *P* can be overcome by employing the magnetoelectric (ME) effects of multiferroic materials, which yields a new type of multilevel nonvolatile magnetoelectric memory.

In previously known nonvolatile memories such as magnetic random access memory (MRAM)[7–10], resistive switching random access memory (RRAM)[11,12], phase change memory (PRAM)[13,14], FeRAM[1–6], and multiferroic or magnetoelectric random access memory (MERAM)[15–23], the digital information is usually stored by three quantities, respectively: the direction of *M* or *P* and the level of resistance (*R*). In addition to *M* and *P*, multiferroic materials that combine magnetism and ferroelectricity[24–28], have a unique physical quantity − the ME coefficient (α), defined by $\alpha_D = \mathrm{d}P/\mathrm{d}H$ and $\alpha_C = \mu_0\,\mathrm{d}M/\mathrm{d}E$, where *H* is magnetic field, and *E* is electric field. The former is called the direct ME effect and the latter is called the converse ME effect. Both α_D and α_C can be either positive or negative, depending on the ME coupling mechanism and the status of *M* and *P*. Therefore, instead of using *M* and *P* themselves to store information, one can employ the ME coefficient to encode digital data. As we demonstrate below, this new concept of memory has many advantages over previously proposed multiferroic memories as well as FeRAM.

Results

Principle and structure of the memory device. For the benefit of easy operations in writing and reading, we consider a multiferroic material (either single-phase or composite) with in-plane *M* and vertical *P*. This

Beijing National Laboratory for Condensed Matter Physics, Institute of Physics, Chinese Academy of Sciences, Beijing 100190, P. R. China. Correspondence and requests for materials should be addressed to Y.S. (email: youngsun@iphy.ac.cn)

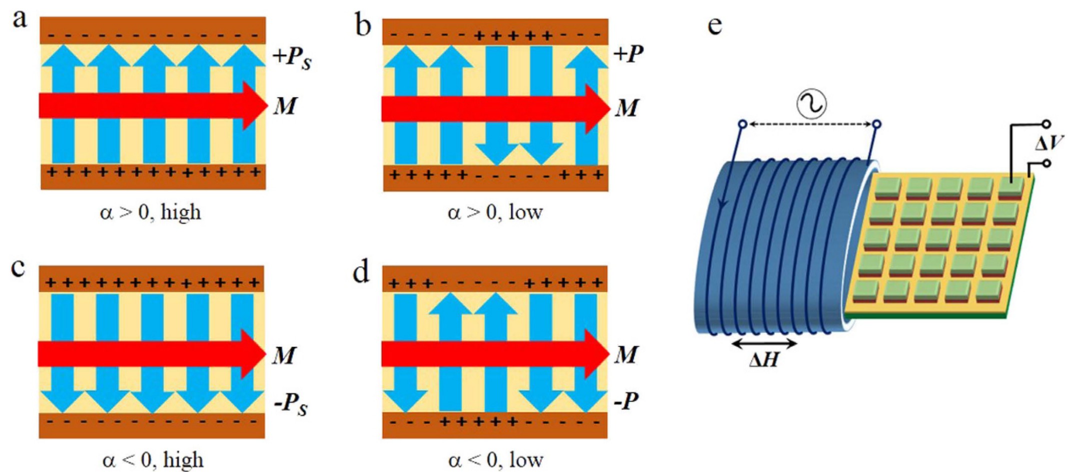

Figure 1. The principle of the multilevel nonvolatile memory. (**a–d**) The schematic of a memory cell showing different states of the ME coefficient α. When the direction of M remains unchanged, the value of α depends on the ratio of up and down ferroelectric domains, ranging from positive to negative. (**e**) The illustration of reading operation. An independent reading coil generates a small ac magnetic field ΔH and the stored information is read out by measuring the induced voltage ΔV. All the memory cells can share a single reading coil, which greatly simplifies the fabrication and operations of the memory device.

multiferroic material is sandwiched between two electrodes to form a memory cell, as shown in Fig. 1. Due to the ME effects in the multiferroic material, a change of in-plane M would induce a change in vertical P, and vice versa. When the direction of M remains unchanged, the sign of $\alpha_D = dP/dH$ depends on the direction of P: $\alpha_D > 0$ for $+P$ (up) and $\alpha_D < 0$ for $-P$ (down). Therefore, we can set $\alpha_D > 0$ as digital "0" and $\alpha_D < 0$ as "1". The digital information is written by applying an electric field between two electrodes to switch the direction of P, like that in FeRAM. To read out information, one simply measures α_D by applying a low H and detecting the induced change of P. In practice, the ME voltage coefficient $\alpha_E = dE/dH \propto \alpha_D$, is measured by applying a low magnetic field (ΔH) and detecting the induced voltage (ΔV) between two electrodes (Fig. 1e) – a technique that has been widely used in the study of multiferroic materials[24–26].

In addition to the conventional two states of polarization (up and down), ferroelectrics have an internal degree of freedom that allows multilevel polarization (MLP) states[5]. As shown in Fig. 1b,d, one can obtain intermediate P states between two saturation values ($+P_S$ and $-P_S$) by adjusting the ratio of up and down ferroelectric domains. Corresponding to different levels of P, the ME coefficient α_E also has different values when the direction of M remains unchanged. Thus, by employing the ME coefficient to store digital data, one can realize not only two-state but also multilevel nonvolatile memories.

To testify the feasibility of above principle, we have performed experiments in a device made of PMN-PT(110)/Terfenol-*D* heterostructure. PMN-PT is a well-known ferroelectric with a large piezoelectric effect and Terfenol-*D* is an important magnetostrictive material with a high magnetostriction constant. Thus, this typical multiferroic heterostructure has pronounced ME coupling via the interfacial strain. Figure 2a plots the structure of the device and the configuration of measurements. The E field is applied between two Ag electrodes to switch the direction of P in PMN-PT layer and the dc magnetic field H_{dc} is applied in plane to control the M of Terfenol-*D* layer. For the measurement of α_E, a conventional dynamic technique is used, where a small ac magnetic field h_{ac} is applied in plane to induce a voltage change between electrodes via the ME effects.

Performance of the memory device. Figure 2b shows how the ME voltage coefficient α_E of the device depends on the status of both M and P. Before measuring α_E, the device was pre-poled by applying a positive or a negative E field of 4 kVcm^{-1} to set the direction of P. Then, α_E was measured as a function of in-plane H_{dc}. When P is set to up (the red curve), α_E is very small in the high H_{dc} region because M is saturated and the magnetostriction coefficient is nearly zero. As H_{dc} decreases from 10 kOe to zero, α_E increases steadily and exhibits a maximum around 1 kOe where the magnetostriction coefficient of Terfenol-*D* is largest. When H_{dc} scans from positive to negative, α_E also changes its sign from positive to negative and shows a minimum around −1 kOe. In contrast, when P is set to down (the black curve), the H dependence of α_E is totally opposite, being negative for $+H_{dc}$ and positive for $-H_{dc}$. These results reveals that the sign of α_E depends on the relative orientation between M and P: when the direction of P is fixed, the sign of α_E can be switched by reversing M with H_{dc}; when the direction of M is fixed, the sign of α_E can be switched by reversing P with external E. The latter case is employed for the memory device because it is more convenient to apply E field in electric circuit.

Though α_E has a maximum with a dc bias field H_{dc} around 1 kOe, it is unfavorable to apply a bias field in practical devices. Thanks to the hysteresis in Fig. 2(b), there is a remanence of α_E at zero bias field. In the following, we focus on the performance of the memory device without a dc bias field.

First, we demonstrate the two-state nonvolatile memory using α_E of the device. After applying an E pulse of +4 kVcm^{-1} to set polarization to $+P_s$, α_E was measured for 100 s; then, another E pulse of −4 kVcm^{-1} was applied

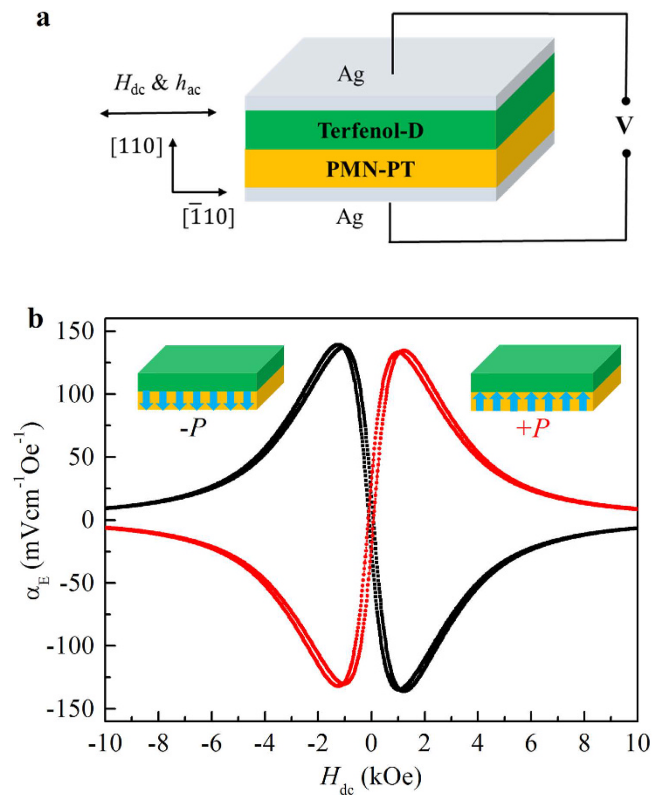

Figure 2. The ME voltage coefficient α_E of a memory device made of the PMN-PT/Terfenol-D multiferroic heterostructure. (**a**) The structure of the device and the measurement configuration. The electric field is applied vertically along [110] of PMN-PT and both the dc bias and ac magnetic fields are applied in plane along [−110] of PMN-PT. (**b**) α_E as a function of dc bias magnetic field with $+P_s$ and $-P_s$, respectively. The state of α_E depends on the relative orientation between *M* and *P*, with the maximums located around ±1 kOe where the magnetostriction coefficient of Terfenol-*D* is largest.

to reverse $+P_s$ to $-P_s$ and α_E was measured for 100 s again. This process was repeated for many cycles. As seen in Fig. 3a, once the applied *E* pulse reverses *P*, α_E inverts its sign and retains the state until the next *E* pulse is applied. Consequently, α_E switches between positive and negative periodically with external *E* pulses. When we reduce the negative *E* field from $-4\,\mathrm{kVcm^{-1}}$ to $-3\,\mathrm{kVcm^{-1}}$, only a small portion of ferroelectric domains are revered. As a result, α_E does not changes its sign to negative but retains a positive low value (Fig. 3b). In this case, α_E switches repeatedly between high and low levels, like the resistance switch in RRAM and PRAM.

Besides the conventional two-state memory, we can achieve multilevel (2^n) non-volatile switch of α_E by carefully selecting the amplitude of -*E* field. Figure 4a,b demonstrate the four-level (2^2) and eight-level (2^3) switch of α_E, respectively. Initially, we apply a $+4\,\mathrm{kVcm^{-1}}$ *E* pulse to set α_E to the positive maximum. Starting from this initial state, we can reach different levels of α_E by applying selective –*E* pulse to either fully or partially reverse the ferroelectric domains. After each *E* pulse, α_E remains its state without apparent decay. Therefore, these well separated levels of α_E ranging from positive to negative constitute an ideal multilevel nonvolatile memory. We note that a reset step by applying $+4\,\mathrm{kVcm^{-1}}$ *E* pulse is required before writing to different levels. This is to refresh the initial state to ensure that the finial state reached by every selective –*E* pulse is reproducible.

Discussion

The above experiments confirm the feasibility of our new principle for multilevel non-volatile memory: the states of the ME coefficient α can be effectively employed to store digital information. Comparing with other known nonvolatile memories, this kind of magnetoelectric memory based on the ME coefficient has many advantages. First, the memory cell has a simple structure so that it is easy to fabricate. Second, the writing operation is achieved rapidly and efficiently, by applying a voltage pulse between two electrodes, just like that in FeRAM and RRAM. Third, the reading operation is much easier than that in conventional FeRAM because it avoids the destructive reading of *P*. Instead, the information is read out by simply measuring the induced voltage across the electrodes while an independent coil supplies a small *H*. Since the reading of ME voltage does not require a minimum area of memory cell, the storage density is not restricted as in conventional FeRAM. Moreover, as illustrated in Fig. 1e, all the memory cells can share a single reading coil and all the stored information can be read out in a parallel way. This greatly simplifies the fabrication and operation of the whole memory device. Fourth, as the device is made of insulating multiferroics and both the writing and reading operations avoid considerable currents, it has a very low power consumption. Finally, compared with the multiple states of resistance in

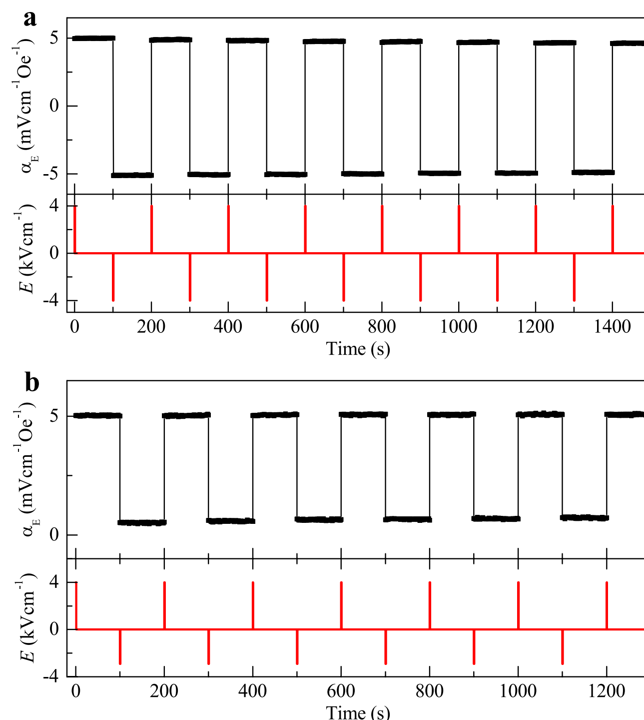

Figure 3. Demonstration of two-level memory. (**a**) Two-level switch of α_E between positive and negative. *E* pulses of $\pm 4\,kVcm^{-1}$ were applied to fully reverse polarization between $+P_s$ and $-P_s$ so that α_E switches between positive and negative. Each *E* pulse lasts for 1 s. (**b**) Two-level switch of α_E between high and low values. *E* pulse of $+4\,kVcm^{-1}$ was used to reach $+P_s$ and $-3\,kVcm^{-1}$ was applied to partially reverse ferroelectric domains. As a result, α_E switches between high and low values.

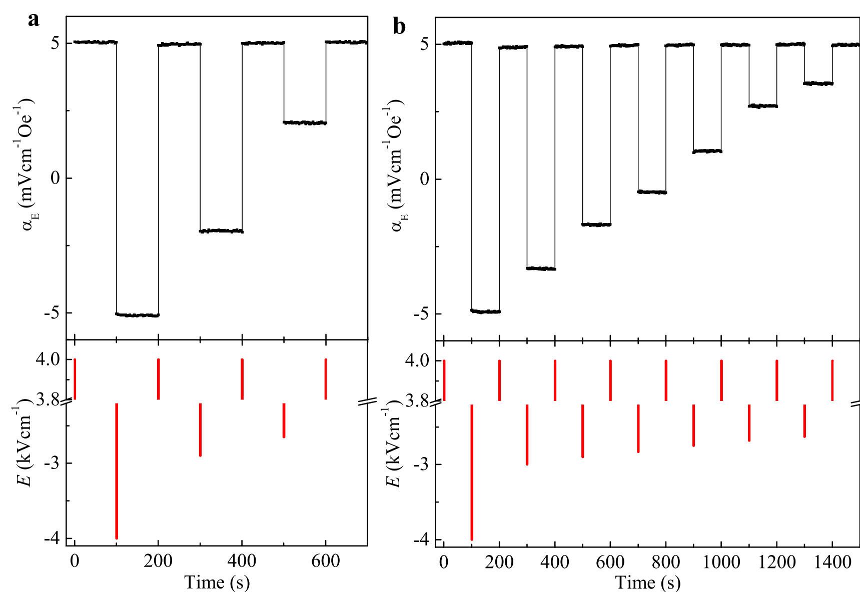

Figure 4. Demonstration of multilevel memory. (**a**) Four-level switch of α_E. (**b**) Eight-level switch of α_E. A reset step with $+4\,kVcm^{-1}$ *E* pulse is performed to refresh the initial state to $+P_s$ before a selective -*E* pulse is applied to reach different levels of α_E. Each *E* pulse lasts for 1 s.

conventional multilevel memories, the multiple levels of the ME coefficient are more distinguishable because it ranges from positive to negative rather than high to low only.

It is worthy to note that the memory device studied in this work has a more fundamental meaning: it is regarded as the fourth memelement, in addition to the memristor, memcapacitor, and meminductor. As discussed in refs 29 and 30, the memory cell exhibiting a pinched or butterfly-shaped hysteresis loop of $\varphi - q$ relationship via the nonlinear ME effects is termed memtranstor. Just like the memristor that has potential applications in nonvolatile memory, the memtranstor also has a great promise in developing next-generation memory devices, as demonstrated in this work.

The principle of using the ME coefficient to store digital information paves a new way towards an ultimate memory. Besides the PMN-PT/Terfenol-*D* heterostructure used in this work, a variety of multiferroic heterostructures and even single-phase multiferroic materials could be used as the memory cell once their ME coefficients can be reliably measured. In the future, a systematical investigation on the selection of materials and design of structures to optimize the performance of this multilevel nonvolatile memory is highly required, with a great promise for industry applications.

Methods

Fabrication of the memory devices. The ferroelectric/ferromagnet multiferroic devices were prepared by using $0.7Pb(Mg_{1/3}Nb_{2/3})O_3$-$0.3PbTiO_3$ (PMN-PT) single-crystal substrate with (110)-cut and $Tb_{0.28}Dy_{0.72}Fe_{1.95}$ (Terfenol-*D*) polycrystalline alloy. Two thin plates of Terfenol-*D* and PMN-PT ($2\,mm \times 2\,mm \times 0.2\,mm$) were bonded together by using a silver epoxy (Epo-Tek H20E, Epoxy Technology Inc.) to form a multiferroic heterostructure. In order to reduce the loss of stress and increase the ME coupling coefficient, the silver epoxy should be thin and hard with a large lap-shear strength. The top and bottom sides of the structure were covered with silver paint (Structure Probe, Inc.) to act as the electrodes. Several devices were made to check the reproducibility of the performance. All devices show the multilevel memory behavior though the magnitude of the ME coefficient is slightly different from sample to sample.

Measurement of the ME voltage coefficient α_E. A conventional dynamic technique was employed to measure the ME coefficient. A Keithley 6221 AC source was used to supply an ac current to the solenoid to generate a small ac magnetic field h_{ac} at a frequency of 100 kHz. In response, a synchronized 100 kHz ac ME voltage, $V_{ac} = x + y$i, across the electrodes was measured by a lock-in amplifier (Stanford Research SR830). The ME voltage coefficient α_E is calculated by $\alpha_E = x/(h_{ac}t)$, where t is the thickness of the ferroelectric layer. To switch the electric polarization of PMN-PT, a Keithley 6517B electrometer was used to apply voltage pulses across the electrodes. The device was loaded in an Oxford TeslatronPT superconducting magnet system to apply the dc bias magnetic field (H_{dc}). All the measurements were performed at 300 K.

References

1. Scott, J. F. & Paz de Araujo, C. A. Ferroelectric memories. *Science* **246,** 1400–1405 (1989).
2. Scott, J. F. *Ferroelectric Memories*, Springer, New York (2000).
3. Park, B. H. *et al.* Lanthanum-substituted bismuth titanate for use in non-volatile memories. *Nature* **401,** 682–684 (1999).
4. Garcia, V. *et al.* Giant tunnel electroresistance for non-destructive readout of ferroelectric states. *Nature* **460,** 81–84 (2009).
5. Lee, D. *et al.* Multilevel data storage memory using deterministic polarization control. *Adv. Mater.* **24,** 402–406 (2012).
6. Guo, R. *et al.* Non-volatile memory based on the ferroelectric photovoltaic effect. *Nature Commun*. **4,** 1990 (2013).
7. Åkerman, J. Toward a universal memory. *Science* **308,** 508–510 (2005).
8. Chappert, C., Fert, A. & Van Dau, F. N. The emergence of spin electronics in data storage. *Nature Mater*. **6,** 813–823 (2007).
9. Parkin, S. S. P., Hayashi, M. & Thomas, L. Magnetic domain-wall racetrack memory. *Science* **320,** 190–194 (2008).
10. Jungwirth, T., Marti, X., Wadley, P. & Wunderlich J. Antiferromagnetic spintronics. *Nature Nanotech*. **11,** 231–241 (2016).
11. Waser, R. & Aono, M. Nanoionics-based resistive switching memories. *Nature. Mater*. **6,** 833–840 (2007).
12. Yang, J. J. *et al.* Memristive switching mechanism for metal/oxide/metal nanodevices. *Nature Nanotech*. **3,** 429–433 (2008).
13. Kolobov, A. V. *et al.* Understanding the phase-change mechanism of rewritable optical media. *Nat. Mater.* **3,** 703–708 (2004).
14. Wuttig, M. & Yamada, N. Phase-change materials for rewriteable data storage. *Nat. Mater.* **6,** 824–832 (2007).
15. Scott, J. F. Multiferroic memories. *Nature Mater*. **6,** 256–257 (2007).
16. Gajek, M. *et al.* Tunnel junctions with multiferroic barriers. *Nature Mater*. **6,** 296–302 (2007).
17. Bibes, M. & Barthélémy, A. Towards a magnetoelectric memory. *Nature Mater*. **7,** 425–426 (2008).
18. Bea, H., Gajek, M., Bibes, M. & Barthelemy, A. Spintronics with multiferroics. *J. Phys. Condens. Matter* **20,** 434231 (2008).
19. Baek, S. H. *et al.* Ferroelastic switching for nanoscale non-volatile magnetoelectric devices. *Nat. Mater.* **9,** 309–314 (2010).
20. Yin, Y. *et al.* Enhanced tunneling electroresistance effect due to a ferroelectrically induced phase transition at a magnetic complex oxide interface. *Nat. Mater.* **12,** 397–402 (2013).
21. Laukhin, V. *et al.* Electric-field control of exchange bias in multiferroic epitaxial heterostructures. *Phys. Rev. Lett.* **97,** 227201 (2006).
22. Wu, S. M. *et al.* Reversible electric control of exchange bias in a multiferroic field-effect device. *Nat. Mater.* **9,** 756–761 (2010).
23. Heron, J. T. *et al.* Deterministic switching of ferromagnetism at room temperature using an electric field. *Nature* **516,** 370–373 (2014).
24. Fiebig, M., Revival of the magnetoelectric effect. *J. Phys. D: Appl. Phys.* **38,** R123–R152 (2005).
25. Eerenstein, W., Mathur, N. D. & Scott, J. F. Multiferroic and magnetoelectric materials. *Nature* **442,** 759–765 (2006).
26. Nan, C.-W. *et al.* Multiferroic magnetoelectric composites: Historical perspective, status, and future directions. *J. Appl. Phys.* **103,** 031101 (2008).
27. Spaldin, N. A., Cheong, S.-W. & Ramesh, R. Multiferroics: Past, present, and future. *Physics Today* **63,** 38–43 (2010).
28. Dong, S., Liu, J.-M., Cheong, S.-W. & Ren, Z. Multiferroic materials and magnetoelectric physics: symmetry, entanglement, excitation, and topology. *Adv. in Phys.* **64,** 519–626 (2015).
29. Shang, D.-S., Chai, Y.-S., Cao, Z.-X., Lu, J. & Sun, Y. Toward the complete relational graph of fundamental circuit elements. *Chin. Phys. B* **24,** 068402 (2015).
30. Shen, J., Cong, J., Chai, Y., Shang, D., Shen, S., Zhai, K., Tian, Y. & Sun Y. Nonvolatile memory based on nonlinear magnetoelectric effects. *Phys. Rev. Applied* **6,** 021001 (2016).

Acknowledgements

This work was supported by the National Key Research Program of China (Grant No. 2016YFA0300700) and the National Natural Science Foundation of China (Grant Nos 11227405, 11534015, 51371192, 11274363), and the Chinese Academy of Sciences (Grants No. XDB07030200 and KJZD-EW-M05).

Author Contributions

Y.S., D.S. and Y.C. conceived the study together. J.S. and J.C. prepared the device and carried out the measurements of the ME coefficient. S.S. and K.Z. assisted in the experiments. All authors involved in discussing and analyzing the data. Y.S. wrote the paper and all authors reviewed the paper.

Additional Information

Competing financial interests: The authors declare no competing financial interests.

How to cite this article: Shen, J. *et al.* A multilevel nonvolatile magnetoelectric memory. *Sci. Rep.* **6**, 34473; doi: 10.1038/srep34473 (2016).

This work is licensed under a Creative Commons Attribution 4.0 International License. The images or other third party material in this article are included in the article's Creative Commons license, unless indicated otherwise in the credit line; if the material is not included under the Creative Commons license, users will need to obtain permission from the license holder to reproduce the material. To view a copy of this license, visit http://creativecommons.org/licenses/by/4.0/

© The Author(s) 2016